ACCEPTED MANUSCRIPT

This "raw" version of the manuscript is being provided to the authors and readers for their technical service. It must be stressed that the manuscript still has to be subjected to copyediting, typesetting, English grammar and syntax corrections, professional editing and authors' review of the galley proof before it is published in its final form. Please note that during these publishing processes, many errors may emerge which could affect the final content of the manuscript and all legal disclaimers applied according to the policies of the Journal.

Synthesis, X-ray structure and DFT calculation of magnetic properties of binuclear Ni(II) complex with tridentate hydrazone-based ligand

TANJA KEŠKIĆ[1], DUŠANKA RADANOVIĆ[1], ANDREJ PEVEC[2], IZTOK TUREL[2],
MAJA GRUDEN, KATARINA ANĐELKOVIĆ, DRAGANA MITIĆ[3], MATIJA ZLATAR[1,*]
and BOŽIDAR ČOBELJIĆ[★]

Faculty of Chemistry, University of Belgrade, Studentski trg 12-16, 11000 Belgrade, Serbia;
*[1]Institute of Chemistry, Technology and Metallurgy, University of Belgrade, Njegoševa 12,
11000 Belgrade, Serbia; [2]Faculty of Chemistry and Chemical Technology, University of
Ljubljana, Večna pot 113, 1000 Ljubljana, Slovenia; [3]Innovation center of the Faculty of
Chemistry, University of Belgrade, Studentski trg 12-16, 11000 Belgrade, Serbia*

Abstract: Binuclear double end-on azido bridged Ni(II) complex (**1**) with composition [Ni$_2$**L**$_2$(μ-$_{1,1}$-N$_3$)$_2$(N$_3$)$_2$]·6H$_2$O, (**L** = (*E*)-*N*,*N*,*N*-trimethyl-2-oxo-2-(2- -(1-(pyridin-2-yl)ethylidene)hydrazinyl)ethan-1-amin) was synthesized and characterized by single-crystal X-ray diffraction method. Ni(II) ions are hexacoordinated with the tridentate heteroaromatic hydrazone-based ligand and three azido ligands (one terminal and two are end-on bridges). DFT calculations revealed that coupling between two Ni(II) centers is ferromagnetic in agreement with binuclear Ni(II) complexes with similar structures.

Keywords: Schiff base; azido-bridged; double end-on.

INTRODUCTION

Azido bridged Ni(II) complexes have received extensive attention from the viewpoint of magnetism and molecular structure, because azido bridges can effectively transmit magnetic coupling, and can give rich structures including binuclear and polynuclear complexes, one-dimensional chainlike complexes, as well as two- and three-dimensional structures.[1–22] Generally speaking, the azido ligand has two typical single or double bridging coordination modes: end-to-end ($\mu_{1,3}$-N$_3$) and end-on ($\mu_{1,1}$-N$_3$) (Scheme 1).[1,3] It has been proven that the end-to-end linking mode usually gives antiferromagnetic interaction, while the end-on mode leads to ferromagnetic interaction, although there are some exceptions.[1,2,5] The angles within the M–(N$_3$)$_n$–M unit are the primary determinant of the type and magnitude of the exchange coupling. The analysis of Ruiz *et al.*[2] performed on bis($\mu_{1,1}$-N$_3$) Ni(II) complexes has predicted ferromagnetic interaction on all ranges of Ni–N(N$_3$)–Ni

angles, with coupling constant *J* increasing upon increasing this angle, yielding a maximum at 104° approximately and then *J* decreases. They have also shown that the bond distance between the metal and bridging atoms has a strong influence on the coupling constant, with the ferromagnetic coupling diminishing upon increasing such distance. Moreover, the out-of-plane displacement of the azido bridge was analyzed to have a negligible influence on the exchange coupling, in contrast to that for hydroxo and alkoxo bridging ligands. In general, in the binuclear Ni(II) complexes with the core formula $[Ni_2(\mu_{1,1}\text{-}N_3)_2]^{2+}$ the mono-, bi-, tri-, or tetradentate ligands complete the coordination spheres of Ni(II) ions.[1,5–20,22] In some cases, the azide anions function as bridging and terminal ligands.[1,7–20,22]
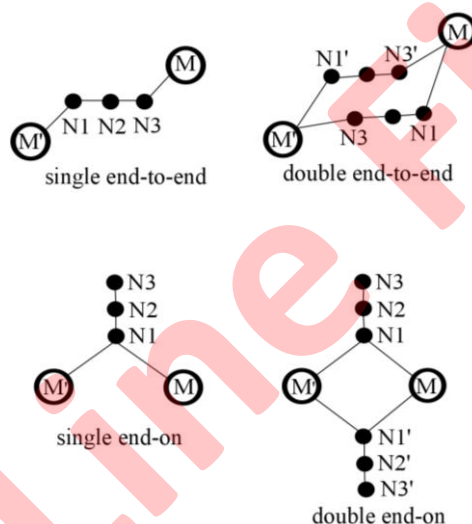
Scheme 1. The most common coordination modes of bridging azido ligands (single and double end-to-end ($\mu_{1,3}\text{-}N_3$) and end-on ($\mu_{1,1}\text{-}N_3$)).

Recently, we have reported the synthesis and magneto-structural characterization of the octahedral binuclear Ni(II) complex $[Ni_2(\mathbf{L^1})_2(\mu_{1,1}\text{-}N_3)_2(N_3)_2]\cdot H_2O\cdot$ $\cdot CH_3OH$[7] ($\mathbf{L^1}$ = (*E*)-*N*,*N*,*N*-trimethyl-2-oxo-2-(2-(quinolin-2-ylmethylene)hydrazinyl)ethan-1-aminium chloride) in which the azide anions function as terminal and bridging ligands. In continuation of our work on azido bridged Ni(II) complexes with heteroaromatic hydrazone based ligands, we report here the synthesis and characterization of new $[Ni_2\mathbf{L}_2(\mu\text{-}_{1,1}\text{-}N_3)_2(N_3)_2]\cdot 6H_2O$ (**1**) (**L** = (*E*)-*N*,*N*,*N*-trimethyl-2-oxo-2-(2-(1-(pyridin-2-yl)ethylidene)hydrazinyl)ethan-1-amin) complex. For the structural characterization of **1,** the IR spectroscopy and X-ray diffraction methods have been used. Furthermore, DFT calculations have been performed to probe magnetic properties (exchange coupling and local zero-field splitting parameters) in **1**.

EXPERIMENTAL

Materials and methods. 2-Acetylpyridine (≥99 %) and Girard's T reagent (99 %) were obtained from Sigma-Aldrich. IR spectra were recorded on a Nicolet 6700 FT-IR spectrometer using the ATR technique in the region 4000−400 cm^{-1} (vs-very strong, s-strong, m-medium, w-weak, bs - broad signal). ^{1}H and ^{13}C NMR spectra were recorded on Bruker Avance 500 spectrometer (^{1}H at 500 MHz; ^{13}C at 125 MHz) at room temperature using TMS as internal standard in DMSO-d^6 (numbering of atoms according to Scheme 1). Chemical shifts are expressed in ppm (δ) values and coupling constants (J) in Hz. Elemental analyses (C, H, and N) were performed by standard micro-methods using the ELEMENTAR Vario ELIII C.H.N.S.O analyzer.

*Synthesis of (E)-N,N,N-trimethyl-2-oxo-2-(2-(1-(pyridin-2-yl)ethylidene)hydrazinyl)eth-an-1-aminium-chloride (**HL**Cl).* The ligand **HL**Cl was synthesized in the reaction of Girard's T reagent (0.84 g, 5.00 mmol) and 2-acetylpyridine (0.56 mL, 5.00 mmol) in methanol (100 mL). The reaction mixture was acidified with 3–4 drops of 2M HCl and refluxed for 120 minutes at 65 °C. The ligand was obtained as a white solid after evaporation of reaction solution at room temperature (~20 °C) during 5 days.

*Synthesis of [Ni$_2$L$_2$(μ-$_{1,1}$-N$_3$)$_2$(N$_3$)$_2$]·6H$_2$O complex (**1**).* Into the solution of ligand **HL**Cl (54 mg, 0.20 mmol) in methanol (10 mL), Ni(BF$_4$)$_2$·6H$_2$O (75 mg, 0.22 mmol) dissolved in H$_2$O (5 mL) and NaN$_3$ (50 mg, 0.46 mmol) was added. Reaction mixture was stirred with heating for 3 h at 75 °C. Green crystals suitable for X-ray analysis arose from the reaction solution after slow evaporation of solvent in refrigerator (~7 ºC) during three weeks.

X-ray crystallography. Crystal data and refinement parameters of compound **1** given in the Supplementary material. X-ray intensity data were collected at 150 K with Agilent SuperNova dual source diffractometer with an Atlas detector equipped with mirror-monochromated Mo $K\alpha$ radiation ($\lambda = 0.71073$ Å). The data were processed using CRYSALIS PRO.[23] The structures were solved by direct methods (SIR-92)[24] and refined by a full-matrix least-squares procedure based on F^2 using SHELXL-2014.[25] All non-hydrogen atoms were refined anisotropically. The water hydrogen atoms were located in a difference map and refined with the distance restraints (DFIX) with O–H = 0.96 Å and with U_{iso}(H) = 1.5 U_{eq}(O). All other hydrogen atoms were included in the model at geometrically calculated positions and refined using a riding model.

Computational details. The exchange coupling constant J of the Heisenberg-Dirac-van Vleck spin-Hamiltonian ($H = -2JS_1S_2$) was calculated with the ORCA program package (version 4.1.2).[26] Broken symmetry DFT formalism [27–31] according to the Yamaguchi approach [32] was used:

$$J = \frac{E_{\text{HS}} - E_{\text{BS}}}{\langle S^2 \rangle_{\text{HS}} - \langle S^2 \rangle_{\text{BS}}}$$

(1)

E_{HS} is the energy of the high-spin, E_{BS} is the energy of the broken-symmetry states; $\langle S^2\rangle_{\text{HS}}$ and $\langle S^2\rangle_{\text{BS}}$ are the corresponding spin expectation values. Scalar relativistic effects were considered at the Zero-Order-Regular-Approximation (ZORA) level.[33] ZORA-def2-TZVP(-f)[34,35] basis set for all atoms have been used. The calculations were performed on the experimentally determined X-ray structure (CCDC 2011514) with M06-2X,[36,37] PWPB95,[38] and B2PLYP[39] exchange-correlation functionals. The chain-of-spheres approximation to the exact exchange (COSX)[40] and the resolution of the identity (RI) approximation[41] in the MP2 part was used. The scalar relativistically reconstructed SARC/J[35,42,43] auxiliary basis sets have been used for

the fitting of the Coulomb integrals, and def2-TZVP/C[44] correlation fitting basis sets were used in the RI-MP2. Positions of hydrogen atoms were optimized, adopting the high-spin state of the binuclear complex, at BP86-D3/def2-TZVP(-f) level of theory.[45–48] Magnetic coupling is rationalized based on the analysis of the overlap of the unrestricted corresponding orbitals [49] from the broken-symmetry determinants.

The individual single-ion zero-field splitting (ZFS) parameters (D and E) in complex **1**, was calculated with two DFT based methods, taking geometry of the binuclear complex and replacing one Ni(II) ion with diamagnetic Zn(II). The first method is the coupled perturbed method (CP)[50,51] at ZORA-BP86/def2-TZVP(-f), CPCM(water) level of theory. The spin-spin contribution was calculated using a restricted spin-density obtained from singly occupied unrestricted natural orbitals.[52] The second method is the ligand-field DFT (LF-DFT) approach by C. Daul *et al.*[53,54] Details about the LF-DFT procedure can be found elsewhere.[55] Briefly, LF-DFT is based on the LF analysis of all the Slater determinants arising from the d^n configuration of the coordinated transition metal ion (45 in the case of Ni(II)) using Kohn-Sham orbitals. LF-DFT calculations are carried out with the ADF program package (version 2017.01)[56–58] at ZORA-OPBE/TZP, COSMO(water) level of theory. The ZFS parameters are deduced using an effective Hamiltonian approach from the lowest eigenvalues and corresponding eigenvectors from LFDFT multiplet calculations in the basis of 0, ±1 M_s wave functions.

RESULTS AND DISCUSSION

Synthesis. The ligand (*E*)-*N*,*N*,*N*-trimethyl-2-oxo-2-(2-(1-(pyridin-2-yl)ethylidene)hydrazinyl)ethan-1-aminium-chloride (**HL**Cl), was obtained in the condensation reaction of 2-acetylpyridine and Girard's T reagent Scheme 2a. Reaction of the ligand **HL**Cl with Ni(BF₄)₂·6H₂O and NaN₃ in excess in methanol/water mixture results in the formation of binuclear double end-on azido bridged Ni(II) complex (**1**) with composition [Ni₂L₂(μ-1,1-N₃)₂(N₃)₂]·6H₂O (Scheme 2b). The ligand **HL**Cl is coordinated in deprotonated form through NNO donor set atoms.
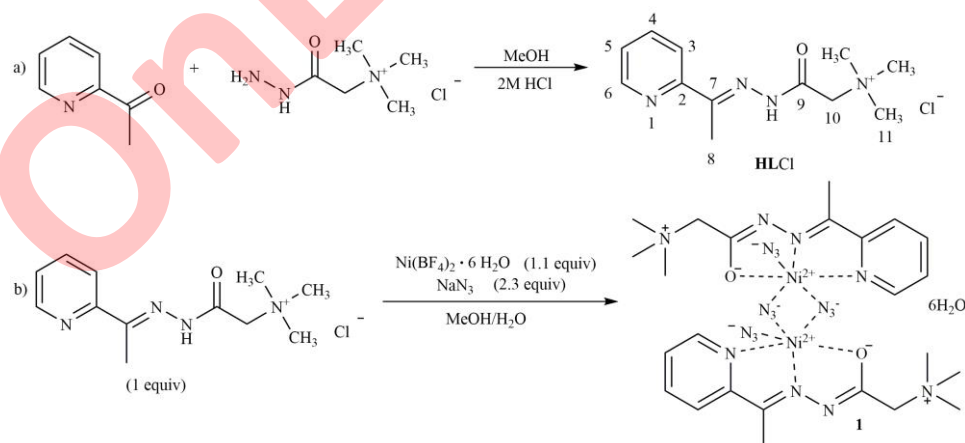
Scheme 2. Synthesis of a) ligand **HL**Cl and b) complex **1**.

*Crystal structure of binuclear [Ni₂**L**₂(μ-₁,₁-N₃)₂(N₃)₂]·6H₂O complex (**1**).* The structure of **1** is depicted in Fig 1. where the numbering scheme adopted for the respective atoms is also given. Selected bond lengths and angles are given in Table I. The complex unit of **1** is a neutral dimer of formula [Ni₂**L**₂(μ-₁,₁--N₃)₂(N₃)₂], which crystallizes in the triclinic crystal system with space group *P*−1 together with six solvent water molecules.
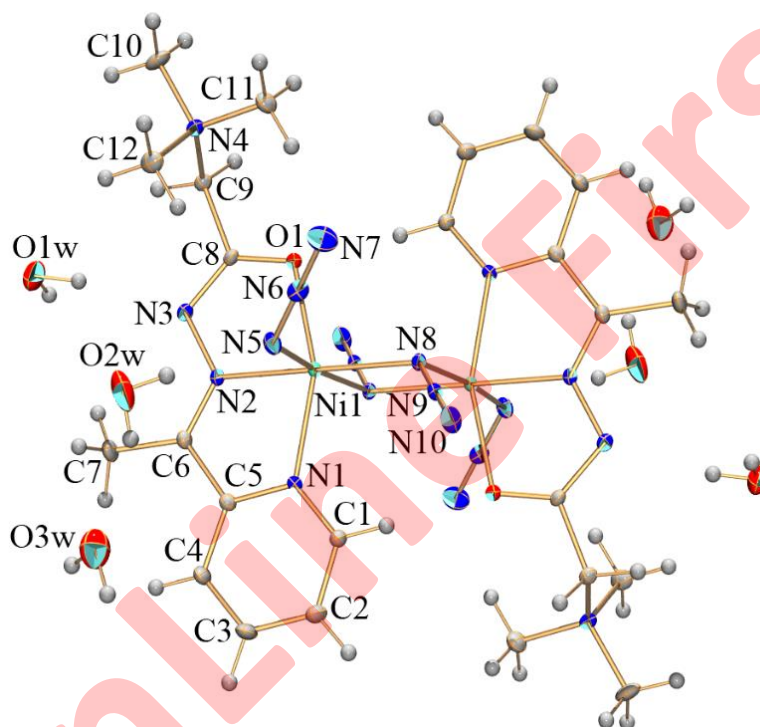

Fig 1. ORTEP presentation of the [Ni₂**L**₂(μ-₁,₁-N₃)₂(N₃)₂]·6H₂O (**1**). Thermal ellipsoids are drawn at the 30 % probability level. Unlabeled part of the dimeric molecule and solvent water molecules are generated by symmetry operation -*x*+1, -*y*, -*z*+1.

In **1**, each Ni(II) center is hexacoordinated with the tridentate heteroaromatic hydrazone-based ligand and three azido ligands (one terminal and the other two are end-on azido bridges). The azido bridges form common edge within the binuclear unit, leading to an edge-sharing bioctahedral structure, while the terminal azido ligands are coordinated in *trans* positions. The N6–N5–Ni1 bond angle of 120.05(18)° shows bent coordination of the anionic terminals. The terminal azido ligands are nearly linear and slightly asymmetric (N5–N6 = 1.195(3) Å and N6–N7 = 1.161(3) Å) with the shorter N(azido)–N(azido) bond further from the metal center. In **1**, **L** is bonded to Ni(II) center through N$_{py}$ (Ni1–N1, 2.077(2) Å), N$_{imine}$ (Ni1–N2, 1.993(2) Å) and O$_{enolate}$ (Ni1–O1, 2.080(2) Å) atoms.

TABLE I. Selected bond lengths and angles for complex **1**.

Bond	Bond length, Å	Angle	Angle, °
Ni1-N1	2.077(2)	N1-Ni1-N2	78.84(8)
Ni1-N2	1.993(2)	N1-Ni1-N5	91.63(9)
Ni1-N5	2.111(2)	N1-Ni1-N8	100.86(8)
Ni1-N8	2.085(2)	N1-Ni1-N8[a]	90.80(8)
Ni1-N8[a]	2.122(2)	N2-Ni1-N5	89.19(9)
Ni1-O1	2.080(2)	N2-Ni1-N8[a]	99.38(8)
N3-C8	1.334(3)	N5-Ni1-N8	90.72(9)
O1-C8	1.268(3)	N8-Ni1-N8[a]	80.72(9)
N5-N6	1.195(3)	N2-Ni1-N8	179.68(8)
N6-N7	1.161(3)	N5-Ni1-N8[a]	171.40(8)
N8-N9	1.208(3)	N2-Ni1-O1	77.55(8)
N9-N10	1.155(3)	N5-Ni1-O1	89.64(9)
		N8-Ni1-O1	102.75(7)
		N8[a]-Ni1-O1	91.45(8)
		N1-Ni1-O1	156.34(8)

Symmetry codes: a = $-x+1$, $-y$, $-z+1$.

   The tridentate coordination mode of each ligand molecule implies the formation of two fused five-membered chelate rings (Ni–N–C–C–N and Ni–N–N–C–O) which are nearly coplanar, as indicated by the dihedral angle of 1.1°. One of the measures of the octahedral strain is average ΔO_h value, defined as the mean deviation of 12 octahedral angles from ideal 90°. The average ΔO_h value calculated for **1** sums 5.97°. The M–L bond lengths in complex **1** have been compared with those observed in $[Ni_2(\mathbf{L^1})_2(\mu_{1,1}\text{-}N_3)_2(N_3)_2]\cdot H_2O\cdot CH_3OH$ ($\mathbf{L^1}$ = ((E)-*N,N,N*-trimethyl-2-oxo-2-(2-(quinolin-2-ylmethylene)hydrazinyl)ethan--1-aminium chloride).[7] The Ni–N$_{quinoline}$ bonds (2.1850(18) Å and 2.1793(19) Å) observed in $[Ni_2(\mathbf{L^1})_2(\mu_{1,1}\text{-}N_3)_2(N_3)_2]\cdot H_2O\cdot CH_3OH$[7] are longer than the Ni–N$_{pyridine}$ (2.077(2) Å) in **1**. Thus, the Ni–N(heterocycles) bond lengths decrease in the order Ni–N(quinoline) > Ni–N(pyridine). The Ni–N$_{imine}$ bond distances observed in **1** and $[Ni_2(\mathbf{L^1})_2(\mu_{1,1}\text{-}N_3)_2(N_3)_2]\cdot H_2O\cdot CH_3OH$[7] are comparable in length 1.993(2) *vs.* 1.9948(17) and 1.9962(18) Å. The Ni–O$_{enolate}$ bond length in **1** (2.080(2) Å) is shorter than the mean Ni–O$_{enolate}$ bond length (2.1185 Å) in $[Ni_2(\mathbf{L^1})_2(\mu_{1,1}\text{-}N_3)_2(N_3)_2]\cdot H_2O\cdot CH_3OH$.[7] The difference in Ni–O(enolate) bond lengths may be attributed to the different weak interactions (electrostatic and dispersion) present in **1** and $[Ni_2(\mathbf{L^1})_2(\mu_{1,1}\text{-}N_3)_2(N_3)_2]\cdot H_2O\cdot CH_3OH$[7] that involve O(enolate) oxygen. Structural parameters correlating the geometry of the central Ni_2N_2 ring of complex **1** are given in Table II. The central ring (Ni_2N_2) is planar with bridging angle (Ni-N$_{azido(end-on)}$–Ni) of 99.28(9)° and Ni···Ni separation of 3.2055(5) Å. The Ni-N$_{azido(end-on)}$ bond distances show a discrepancy of 0.037 Å. In the analyzed complex, the out-of-plane deviation (δ) of the azide anions is 36.8(2)°. The Ni-N$_{azido(end-on)}$–Ni bond angle, the Ni–N$_{azido(end-on)}$ bond lengths and Ni···Ni distance

observed in binuclear complex **1** fit into the range of values obtained for the ferromagnetically coupled binuclear tetraazido Ni(II) complexes with tridentate or bis-tridentate ligands.[7–20] The positions of the terminal azido ligands with respect to the Ni_2N_2 plane are defined by the $N_{azido(terminal)}$–Ni–$N_{azido(end-on)}$–Ni torsion angles.

TABLE II. Structural parameters correlating the geometry of the central Ni_2N_2 ring of binuclear complex **1**.

Complex	Angle, °	Distace, Å		Dihedral angel, °	δ^a / °
	Ni–$N_{azido(end-on)}$–Ni	Ni···Ni	Ni–$N_{azido(end-on)}$	$N_{azido(terminal)}$–Ni–$N_{azido(end-on)}$–Ni	
(**1**)	99.28(9)	3.2055(5)	2.122(2); 2.085(2)	5.7(6); −179.15(9)	36.8(2)

$^a\delta$ is the out-of-plane deviation of the azide ion measured as the angle between Ni_2N_2 plane and the N–N bond.

In the crystals of **1**, the dimers are assembled into the three-dimensional supramolecular structure through intermolecular hydrogen bonds. The solvent water molecules mediate in connecting the Ni(II) dimers into the layer parallel with the (001) lattice plane through intermolecular hydrogen bonds: Ow–H···Ow, Ow–H···N_{azide} and Ow–H···N_{amide}, Table S-2, Fig S-1a. The neighboring layers are linked through weak intermolecular C–H···N_{azide} hydrogen bonds, Table S-2, Fig S-1b. Besides, a weak intermolecular contact of C–H···π(py) type with H···Cg(py) of 3.130 Å (Cg is the center of gravity of the pyridine ring) which connects the dimers along *b* crystallographic direction has been observed (Fig S-1c). The solvent water molecules O1W, O2W, and O3W fill the channels which were found to extend parallel with *a* crystallographic direction (Fig S-1b).

Exchange coupling. The exchange coupling in binuclear complex **1** has been calculated by the broken-symmetry DFT approach[27–31] with M06-2X, B2PLYP, and PWPB95 functionals (Table III) revealing ferromagnetic coupling between Ni(II) centers regardless of the exchange-correlation functional. *J* coupling calculated with double-hybrid functionals without perturbational correction, *i.e.,* DFT only values (Table III), are similar to the calculated values by M06-2X.

TABLE III. Exchange coupling constant (*J*) calculated by the broken-symmetry DFT approach with meta-hybrid M06-2X and double-hybrid B2PLYP and PWPB95 for Ni(II) binuclear complex **1**. DFT only values for double-hybrids are given as well.

DFT	J / cm^{-1}
M06-2X	2 6.72
B2PLYP (DFT)	31.35
B2PLYP	19.24
PWPB95 (DFT)	29.77
PWPB95	19.40

The reason is the high admixture of the exact exchange in all three exchange-correlation functionals – 54 % in M06-2X, 53 % in B2PLYP, and 50 % in PWPB95. Perturbational contribution to the exchange coupling brings the antiferromagnetic

contribution, hence lower the calculated *J*. Calculated *J* coupling constant fit into the range of values obtained for the ferromagnetically coupled binuclear tetraazido Ni(II) complexes with tridentate or bis-tridentate ligands (1.9-36 cm^{-1}).[7–20]

Ni(II) ions are in local S=1 electronic state in octahedral coordination. Localized single occupied molecular orbitals are of local d_{x2-y2} and d_{z2} character (Fig 2). Calculated ferromagnetic coupling is a consequence of the poor overlap of the pairs of magnetic orbitals (Fig. 2). The calculated overlap is 0.00010 for the first pair and 0.00098 for the second pair. Such insignificant overlaps indicate that the antiferromagnetic coupling is suppressed.[59]
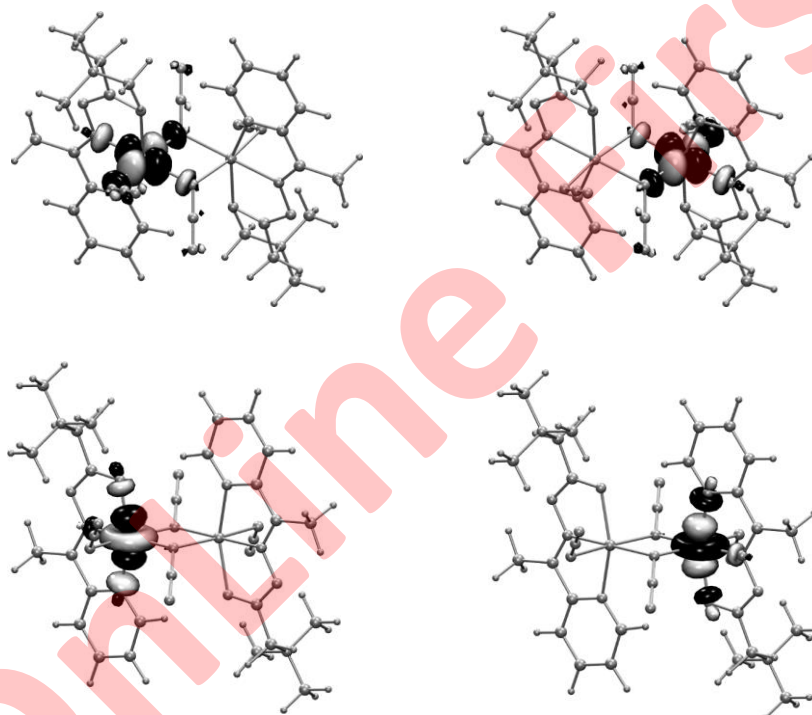

Fig 2. Localized magnetic orbitals of **1**. Isosurfaces were drawn at 0.04 e/Å^3.

Local Zero-Field-Splitting. Local ZFS parameters (*D* and *E*) are calculated with two DFT based methods (CP-DFT[50,51] and LF-DFT[53,54]) by replacing one Ni(II) ion with closed-shell Zn(II),[60,61] Table IV. Both methods give comparable results, with LF-DFT giving slightly larger values. The trend in calculated ZFS parameters with these two methods is the same as previously observed for mononuclear Mn(IV) complexes.[62] LF-DFT is better suited for the cases where near degeneracy is present, *i.e.* when excitation energies are too small for perturbational methods.[55,63] In contrast, CP-DFT is more convenient when metal-ligand covalency is large.[64] Spin-spin contributions to the ZFS parameters, as

calculated by CP-DFT, are negligible (0.02 cm^{-1} to D and -0.01 to E). The results are as expected for close to perfect octahedral coordination.[65,66] The extent of distortion from ideal octahedron is evaluated by the continuous shape measures (CShMs)[67,68] calculated with SHAPE 2.1. CShM values, presenting the deviation from ideal octahedron, is 1.668, in line with the ΔO_h value of 5.97.

TABLE IV. Calculated individual local ZFS parameters D and E for **1**, with CP-DFT and LF-DFT methods

	CP-DFT	LF-DFT
D / cm^{-1}	–0.63	–1.36
E / cm^{-1}	–0.16	–0.12
E / D	0.25	0.09

CONCLUSION

Herein, the synthesis and X-ray characterization of new [Ni$_2$**L**$_2$(μ-$_{1,1}$--N$_3$)$_2$(N$_3$)$_2$]·6H$_2$O (**1**) (**L** = (*E*)-*N*,*N*,*N*-trimethyl-2-oxo-2-(2-(1-(pyridin-2-yl)ethyl-idene)hydrazinyl)ethan-1-amin) complex is presented. Binuclear complex **1** crystallizes as the hexahydrate in the triclinic crystal system with space group *P*−1. Ni(II) centers are hexacoordinated with the tridentate heteroaromatic hydrazone-based ligand, one terminal azido ligand, and two end-on azide bridged ligands. Broken-symmetry DFT calculations based on the X-ray crystal structure of **1** indicate the ferromagnetic coupling between the metal centers, irrespectively of the exchange-correlation functional employed. Ferromagnetic coupling is characteristic of the double end-on azide bridged binuclear Ni(II) complexes.[1,2] Calculated magnetic coupling is in accordance with the range of values obtained for the structurally similar, ferromagnetically coupled binuclear tetraazido Ni(II) complexes.[7–20] Furthermore, the computational study of magnetic properties of **1** is supplemented with calculations of local zero-field parameters.

SUPPLEMENTARY MATERIAL

The additional data are available electronically at the pages of journal website: http:////www.shd.org.rs/JSCS/, or from the corresponding author on request.

Additional crystallographic data for the structure reported in this paper have been deposited at the Cambridge Crystallographic Data Centre with quotation number CCDC 2011514 and is available free of charge on request via www.ccdc.cam.ac.uk/data_request/cif.

ИЗВОД

СИНТЕЗА, КРИСТАЛНА СТРУКТУРА И ПРОРАЧУНИ ФУНКЦИОНАЛА ГУСТИНЕ МАГНЕТНИХ СВОЈСТАВА БИНУКЛЕАРНОГ КОМПЛЕКСА Ni(II) СА ТРИДЕНТАТНИМ ХИДРАЗОНСКИМ ЛИГАНДОМ

ТАЊА КЕШКИЋ, ДУШАНКА РАДАНОВИЋ[1], АНДРЕЈ ПЕВЕЦ[2], ИЗТОК ТУРЕЛ[2], МАЈА ГРУДЕН, КАТАРИНА АНЂЕЛКОВИЋ, ДРАГАНА МИТИЋ[4], МАТИЈА ЗЛАТАР[1] и БОЖИДАР ЧОБЕЉИЋ

Хемијски факулῐеῐ, Универзиῐеῐ у Беоīраду, Сῐуденῐски ῐрī 12–16, 11000 Беоīрад, Србија; [1]Инсῐиῐуῐ за хемију, ῐехнолоīију и меῐалурīију, Универзиῐеῐ у Беоīраду, Њеīошева 12, 11000 Беоīрад, Србија; [2]Факулῐеῐ за хемију и хемијску ῐехнолоīију, Универзиῐеῐ у Љубљани, Вечна йоῐ 113, 1000 Љубљана, Словенија; [3] Иновациони ценῐар Хемијскоī факулῐеῐа, Универзиῐеῐ у Беоīраду, Сῐуденῐски ῐрī 12–16, 11000 Беоīрад, Србија

Синтетисан је и окарактерисан рендгенском структурном анализом бинуклеарни end-on азидом премошћени комплекс Ni(II) састава [Ni$_2$**L**$_2$(μ-$_{1,1}$-N$_3$)$_2$(N$_3$)$_2$]·6H$_2$O, (**L** = (*E*)-*N*,*N*,*N*- -триметил-2-оксо-2-(2-(1-(пиридин-2-ил)етилиден)хидразинил)етан-1-амин). Јони Ni(II) су хексакоординовани преко тридентатног хетероароматичног хидразонског лиганда и три азидо лиганда (од којих је један терминални а два су end-on мосна). Прорачуни функционала густине су показали да између два Ni(II) центра постоји феромагнетно купловање што је у сагласности са бинуклеарним комплексима Ni(II) сличних структура.

(Примљено 25. јуна; прихваћено 1. јула 2020)

REFERENCES

1. J. Ribas, A. Escuer, M. Monfort, R. Vicente, R. Corteś, L. Lezama, T. Rojo, *Coord. Chem. Rev.* **193–195** (1999) 1027–1068 (https://doi.org/10.1016/S0010-8545(99)00051-X)
2. E. Ruiz, J. Cano, S. Alvarez, P. Alemany, *J. Am. Chem. Soc.* **120** (1998) 11122–11129 (https://pubs.acs.org/doi/abs/10.1021/ja981661n)
3. A. Escuer, G. Aromí, *Eur. J. Inorg. Chem.* (2006) 4721–4736 (https://doi.org/10.1002/ejic.200600552)
4. F.-C. Liu, Y.-F. Zeng, J.-R. Li, X.-H. Bu, H.-J. Zhang, J. Ribas, *Inorg. Chem.* **44** (2005) 7298–7300 (https://pubs.acs.org/doi/abs/10.1021/ic051030b)
5. P. Chaudhuri, R. Wagner, S. Khanra, T. Weyhermüller, *Dalton Trans.* (2006) 4962–4968 (https://doi.org/10.1039/B610308A)
6. J. Ribas, M. Monfort, C. Diaz, C. Bastos, X. Solans, *Inorg. Chem.* **33** (1994) 484–489 (https://doi.org/10.1021/ic00081a015)
7. M. Č. Romanović, B. R. Čobeljić, A. Pevec, I. Turel, V. Spasojević, A. A. Tsaturyan, I. N. Shcherbakov, K. K. Anđelković, M. Milenković, D. Radanović, M. R. Milenković, *Polyhedron* **128** (2017) 30–37 (https://doi.org/10.1016/j.poly.2017.02.039)
8. S. Sarkar, A. Mondal, M.S. El Fallah, J. Ribas, D. Chopra, H. Stoeckli-Evans, K.K. Rajak, *Polyhedron* **25** (2006) 25–30 (https://doi.org/10.1016/j.poly.2005.06.059)
9. H.-D. Bian, W. Gu, Q. Yu, S.-P. Yan, D.-Z. Liao, Z.-H. Jiang, P. Cheng, *Polyhedron* **24** (2005) 2002– 2008 (https://doi.org/10.1016/j.poly.2005.06.011)
10. S. Liang, Z. Liu, N. Liu, C. Liu, X. Di, J. Zhang, *J. Coord. Chem.* **63** (2010) 3441–3452 (https://doi.org/10.1080/00958972.2010.512386)
11. S.S. Massoud, F.R. Louka, Y.K. Obaid, R. Vicente, J. Ribas, R.C. Fischer, F.A. Mautner, *Dalton Trans.* **42** (2013) 3968–3978 (https://pubs.rsc.org/en/content/articlelanding/2013/dt/c2dt32540c)
12. R. Cortés, J.I. Ruiz de Larramendi, L. Lezama, T. Rojo, K. Urtiaga, M.I. Arriortua, *J. Chem. Soc. Dalton Trans.* (1992) 2723–2728 (https://doi.org/10.1039/DT9920002723)

13. M.G. Barandika, R. Cortés, L. Lezama, M.K. Urtiaga, M.I. Arriortua, T. Rojo, *J. Chem. Soc., Dalton Trans.* (1999) 2971−2976 (https://doi.org/10.1039/A903558C)
14. A. Escuer, R. Vicente, J. Ribas, X. Solans, *Inorg. Chem*. **34** (1995) 1793–1798 (https://doi.org/10.1021/ic00111a029)
15. A. Solanki, M. Monfort, S.B. Kumar, *J. Mol. Struct*. **1050** (2013) 197–203 (https://doi.org/10.1016/j.molstruc.2013.07.036)
16. S. Nandi, D. Bannerjee, J.-S. Wu, T.-H. Lu, A.M.Z. Slawin, J.D. Woollins, J. Ribas, C. Sinha, *Eur. J. Inorg. Chem.* (2009) 3972–3981 (https://doi.org/10.1002/ejic.200900423)
17. A. R. Jeong, J. W. Shin, J. H. Jeong, K. H. Bok, C. Kim, D. Jeong, J. Cho, S. Hayami, K. S. Min, *Chem. Eur. J*. **23** (2017) 3023–3033 (https://doi.org/10.1002/chem.201604498)
18. A. R. Jeong, J. Choi, Y. Komatsumaru, S. Hayami, K. S. Min, *Inorg. Chem. Commun*. **86** (2017) 66–69 (https://doi.org/10.1016/j.inoche.2017.09.023)
19. S. Deoghoria, S. Sain, M. Soler, W.T. Wong, G. Christou, S.K. Bera, S.K. Chandra, *Polyhedron* **22** (2003) 257–262 (https://doi.org/10.1016/S0277-5387(02)01336-0)
20. S. Sain, S. Bid, A. Usman, H.-K. Fun, G. Aromí, X. Solans, S.K. Chandra, *Inorg. Chim. Acta* **358** (2005) 3362–3368 (https://doi.org/10.1016/j.ica.2005.05.011)
21. A. N. Georgopoulou, C. R. Raptopoulou, V. Psycharis, R. Ballesteros, B. Abarca, A. K. Boudlais, *Inorg. Chem*. **48** (2009) 3167–3176 (https://doi.org/10.1021/ic900115c)
22. H.-Z. Kou, S. Hishiya, O. Sato, *Inorg. Chim. Acta* **361** (2008) 2396–2406 (https://doi.org/10.1016/j.ica.2007.12.018)
23. Oxford Diffraction, CrysAlis PRO Software system, Oxford Diffraction Ltd., Yarnton (England) 2009.
24. A. Altomare, G. Cascarano, C. Giacovazzo, A. Guagliardi, *J. Appl. Crystallogr*. **26** (1993) 343-350 (https://doi.org/10.1107/S0021889892010331)
25. G. M. Sheldrick, *Acta. Crystallogr*. **A64** (2008) 112–122 (https://doi.org/10.1107/S0108767307043930)
26. F. Neese, *Wiley Interdiscip. Rev. Comput. Mol. Sci.* **2** (2012) 73–78. (https://doi.org/10.1002/wcms.81)
27. G. Jonkers, C. A. de Lange, L. Noodleman, E. J. Baerends, *Mol. Phys*. **46** (1982) 609–620 (https://doi.org/10.1080/00268978200101431)
28. L. Noodleman, *J. Chem. Phys*. **74** (1981) 5737–5743 (https://doi.org/10.1063/1.440939)
29. L. Noodleman, E. R. Davidson, *Chem. Phys*. **109** (1986) 131–143 (https://doi.org/10.1016/0301-0104(86)80192-6)
30. L. Noodleman, J. G. Norman, J. H. Osborne, A. Aizman, D. A. Case, *J. Am. Chem. Soc.* **107** (1985) 3418–3426 (https://doi.org/10.1021/ja00298a004)
31. F. Neese, *Coord. Chem. Rev.* **253** (2009) 526–563 (https://doi.org/10.1016/j.ccr.2008.05.014)
32. T. Soda, Y. Kitagawa, T. Onishi, Y. Takano, Y. Shigeta, H. Nagao, Y. Yoshioka, K. Yamaguchi, *Chem. Phys. Lett.* **319** (2000) 223–230 (https://doi.org/10.1016/S0009-2614(00)00166-4)
33. C. van Wüllen, *J. Chem. Phys*. **109** (1998) 392–399 (https://doi.org/10.1063/1.476576)
34. F. Weigend, R. Ahlrichs, *Phys. Chem. Chem. Phys.* **7** (2005) 3297–3305 (https://doi.org/10.1039/b508541a)
35. D. A. Pantazis, X.-Y. Chen, C. R. Landis, F. Neese, *J. Chem. Theory Comput.* **4** (2008) 908–919 (https://doi.org/10.1021/ct800047t)
36. Y. Zhao, D. G. Truhlar, *J. Chem. Phys.* **125** (2006) 194101 (https://doi.org/10.1063/1.2370993)

37. Y. Zhao, D. G. Truhlar, *Theor. Chem. Acc.* **120** (2008) 215–241
    (https://doi.org/10.1007/s00214-007-0310-x)
38. L. Goerigk, S. Grimme, *J. Chem. Theory Comput.* **7** (2010) 291–309
    (https://doi.org/10.1021/ct100466k)
39. S. Grimme, *J. Chem. Phys.* **124** (2006) 034108 (https://doi.org/10.1063/1.2148954)
40. F. Neese, F. Wennmohs, A. Hansen, U. Becker, *Chem. Phys.* **356** (2009) 98–109
    (https://doi.org/10.1016/j.chemphys.2008.10.036)
41. F. Neese, *J. Chem. Phys.* **115** (2001) 11080–11096 (https://doi.org/10.1063/1.1419058)
42. D. A. Pantazis, F. Neese, *J. Chem. Theory Comput.* **5** (2009) 2229–2238
    (https://doi.org/10.1021/ct900090f)
43. F. Weigend, *Phys. Chem. Chem. Phys.* **8** (2006) 1057–1065
    (https://doi.org/10.1039/b515623h)
44. A. Hellweg, C. Hättig, S. Höfener, W. Klopper, *Theor. Chem. Acc.* **117** (2007) 587–597
    (https://doi.org/10.1007/s00214-007-0250-5)
45. A. D. Becke, *Phys. Rev. A* **38** (1988) 3098–3100
    (https://doi.org/10.1103/PhysRevA.38.3098)
46. J. P. Perdew, *Phys. Rev. B* **33** (1986) 8822–8824
    (https://doi.org/10.1103/PhysRevB.33.8822)
47. S. Grimme, J. Antony, S. Ehrlich, H. Krieg, *J. Chem. Phys.* **132** (2010) 154104
    (https://doi.org/10.1063/1.3382344)
48. S. Grimme, S. Ehrlich, L. Goerigk, *J. Comput. Chem.* **32** (2011) 1456–1465
    (https://doi.org/10.1002/jcc.21759)
49. F. Neese, *J. Phys. Chem. Solids* **65** (2004) 781–785
    (https://doi.org/10.1016/J.JPCS.2003.11.015)
50. F. Neese, E. I. Solomon, *Inorg. Chem.* **37** (1998) 6568–6582
    (https://doi.org/10.1021/ic980948i)
51. F. Neese, *J. Chem. Phys.* **127** (2007) 164112 (https://doi.org/10.1063/1.2772857)
52. S. Sinnecker, F. Neese, *J. Phys. Chem. A* **110** (2006) 12267–12275
    (https://doi.org/10.1021/jp0643303)
53. M. Atanasov, C. A. A. Daul, C. Rauzy, *Chem. Phys. Lett.* **367** (2003) 737–746
    (https://doi.org/10.1016/S0009-2614(02)01762-1)
54. M. Atanasov, C. A. Daul, C. Rauzy, *A DFT based ligand field theory*, in D. M. P.
    Mingos, T. Schönherr (Eds.), *Opt. Spectra Chem. Bond. Inorg. Compd.*, Springer Berlin
    Heidelberg, Berlin, Heidelberg, 2004, pp. 97–125 (https://doi.org/10.1007/b11308)
55. D. Darmanović, I. N. Shcherbakov, C. Duboc, V. Spasojević, D. Hanžel, K. Anđelković,
    D. Radanović, I. Turel, M. Milenković, M. Gruden, B. Čobeljić, M. Zlatar, *J. Phys.
    Chem. C* (2019) (https://doi.org/10.1021/acs.jpcc.9b08066)
56. G. te Velde, F. M. Bickelhaupt, E. J. Baerends, C. Fonseca Guerra, S. J. A. van
    Gisbergen, J. G. Snijders, T. Ziegler, *J. Comput. Chem.* **22** (2001) 931–967
    (https://doi.org/10.1002/jcc.1056)
57. C. Fonseca Guerra, J. G. Snijders, G. te Velde, E. J. Baerends, *Theor. Chem. Accounts
    Theory, Comput. Model. (Theoretica Chim. Acta)* **99** (1998) 391–403
    (https://doi.org/10.1007/s002140050353)
58. ADF2017, SCM, Theoretical Chemistry, Vrije Universiteit, Amsterdam, The
    Netherlands, https://www.scm.com
59. D. A. Pantazis, V. Krewald, M. Orio, F. Neese, *Dalt. Trans.* **39** (2010) 4959–4967
    (https://doi.org/10.1039/c001286f)

60. F. El-Khatib, B. Cahier, F. Shao, M. López-Jordà, R. Guillot, E. Rivière, H. Hafez, Z. Saad, J. J. Girerd, N. Guihéry, T. Mallah, *Inorg. Chem.* **56** (2017) 4601–4608 (https://doi.org/10.1021/acs.inorgchem.7b00205)
61. I. Nemec, R. Herchel, M. Machata, Z. Trávníček, *New J. Chem.* **41** (2017) 11258–11267 (https://doi.org/10.1039/c7nj02281f)
62. M. Zlatar, M. Gruden, O. Vassilyeva, E. Buvaylo, A. Ponomaryov, S. Zvyagin, J. Wosnitza, J. Krzystek, P. García-Fernández, C. Duboc, *Inorg. Chem.* **55** (2016) 1192–1201 (https://doi.org/10.1021/acs.inorgchem.5b02368)
63. M. Gruden-Pavlović, M. Perić, M. Zlatar, P. García-Fernández, *Chem. Sci.* **5** (2014) 1453–1462 (https://doi.org/10.1039/C3SC52984C)
64. L. Wang, M. Zlatar, F. Vlahović, S. Demeshko, C. Philouze, F. Molton, M. Gennari, F. Meyer, C. Duboc, M. Gruden, *Chem. - A Eur. J.* **24** (2018) 11973–11982 (https://doi.org/10.1002/chem.201705989)
65. S. Gómez-Coca, D. Aravena, R. Morales, E. Ruiz, *Coord. Chem. Rev.* **289**–**290** (2015) 379–392 (https://doi.org/10.1016/J.CCR.2015.01.021)
66. A. K. Bar, C. Pichon, J.-P. Sutter, *Coord. Chem. Rev.* **308** (2016) 346–380 (https://doi.org/10.1016/J.CCR.2015.06.013)
67. M. Pinsky, D. Avnir, **37** (1998) 5575–5582 (https://doi.org/10.1021/IC9804925)
68. S. Alvarez, P. Alemany, D. Casanova, J. Cirera, M. Llunell, D. Avnir, *Coord. Chem. Rev.* **249** (2005) 1693–1708 (https://doi.org/10.1016/J.CCR.2005.03.031)
.

Synthesis, X-ray structure and DFT calculation of magnetic properties of binuclear Ni(II) complex with tridentate hydrazone-based ligand

TANJA KEŠKIĆ, DUŠANKA RADANOVIĆ[1], ANDREJ PEVEC[2], IZTOK TUREL[2], MAJA GRUDEN, KATARINA ANĐELKOVIĆ, DRAGANA MITIĆ[3], MATIJA ZLATAR[1] and BOŽIDAR ČOBELJIĆ[★]

Faculty of Chemistry, University of Belgrade, Studentski trg 12-16, 11000 Belgrade, Serbia; [1]Institute of Chemistry, Technology and Metallurgy, University of Belgrade, Njegoševa 12, 11000 Belgrade, Serbia; [2]Faculty of Chemistry and Chemical Technology, University of Ljubljana, Večna pot 113, 1000 Ljubljana, Slovenia; [3]Innovation center of the Faculty of Chemistry, University of Belgrade, Studentski trg 12-16, 11000 Belgrade, Serbia

ISOLATED YIELDS AND SPECTROSCOPIC DATA OF SYNTHESIZED COMPOUNDS

*(E)-N,N,N-trimethyl-2-oxo-2-(2-(1-(pyridin-2-yl)ethylidene)hydrazinyl)ethan-1-aminium-chloride (**HL**Cl).* Yield 1.17 g (87%). White solid. IR (ATR, cm^{-1}): 3387w, 3127m, 3090m, 3049m, 3016m, 2950s, 1700vs, 1612w, 1549s, 1485m, 1400m, 1300w, 1253w, 1200s, 1153w, 1135m, 1095w, 1073m, 975w, 944w, 914m, 748w, 683w. Anal. Calcd. for $C_{12}H_{19}ClN_4O$ (*FW*: 270.76): C, 53.23; H, 7.07; N, 20.69 %. Found: C, 53.34; H, 7.38; N, 20.49 %. ^{1}H NMR: 11.41 (N-H, s), 4.92 (C10-H$_2$, s), 3.35 (C11-H$_9$, s), 2.37 (C8-H$_3$, s), 8.62 (C3-H, m), 7.45 (C4-H, m), 7.91 (C5-H, td, $J^3 = 10$ Hz, $J^4 = 5$ Hz), 8.12 (C6-H, d, $J^3 = 10$ Hz). ^{13}C NMR: 63.2 (C10), 53.7 (C11), 13.9 (C8), 149.2 (C3), 124.9 (C4), 137.2 (C5), 120.8 (C6), 154.9 (C7), 155.3 (C2), 167.1 (C9).

*[Ni$_2$**L**$_2$(μ-$_{1,1}$-N$_3$)$_2$(N$_3$)$_2$]·6H$_2$O complex (**1**).* Yield 126 mg (73 %). IR (ATR, cm^{-1}): 3344s, 3036w, 2039vs, 1619w, 1595w, 1540s, 1469m, 1441m, 1399w, 1335w, 1300m, 1247w, 1200w, 1145w, 1074w, 1026w, 973w, 909w, 781w, 750w, 676w, 571w. Anal. Calcd. for $C_{24}H_{48}N_{20}Ni_2O_8$ (*FW*: 862.24): C, 33.43; H, 5.61; N 32.49 %. Found: C, 33.31; H, 5.69; N 32.24.

SUPPORTING INFORMATION FOR X-RAY CRYSTALOGRAPHY

TABLE S-1. Crystal data and structure refinement details for **1**.

	1
Empirical formula	$C_{24}H_{48}N_{20}Ni_2O_8$
FW / g mol^{-1}	862.24
Crystal size, mm	$0.20 \times 0.20 \times 0.05$
Crystal color	yellow
Crystal system	triclinic
Space group	*P* –1
a / Å	8.9538(7)
b / Å	9.0014(6)
c / Å	13.1769(11)
α / °	76.170(6)
β / °	73.159(7)
γ / °	82.598(6)
Volume, Å^3	984.97(14)
Z	1
Calculated density, g cm^{-3}	1.454
F(000)	452
Reflections collected	9259
Independent reflections	5142
R_{int}	0.0420
Reflections observed	4217
Parameters	266
Final *R* indices [$I > 2\sigma (I)$]^a	0.0495
wR_2 (all data)^b	0.1314
Goof, S^c	1.039
Maximum/minimum residual electron density, e Å^{-3}	+1.65/–0.65

^{a} $R = \sum||F_o| - |F_c||/\sum|F_o|$. ^{b} $wR_2 = \{\sum[w(F_o^2 - F_c^2)^2]/\sum[w(F_o^2)^2]\}^{1/2}$.
^{c} $S = \{\sum[w(F_o^2 - F_c^2)^2]/(n/p)\}^{1/2}$ where *n* is the number of reflections and *p* is the total number of parameters refined.

TABLE S-2. Hydrogen-bond parameters for complex **1**.

| D–H···A	Distance, Å			Angle, °	Symm. operation on A
	D–H	H···A	D···A	D–H···A	
O1W–H1W···N3	0.86(5)	2.13(5)	2.982(4)	171(4)	
O2W–H3W···N5	0.84(4)	2.04(4)	2.885(4)	177(5)	
O2W–H4W···O3W	0.84(5)	1.97(5)	2.726(5)	150(5)	
O3W–H5W···N7	0.85(4)	2.18(4)	2.992(5)	160(5)	x, 1+y, z
O3W–H6W···O1W	0.86(4)	1.96(4)	2.748(5)	153(6)	1+x, y, z
Intra C1–H1···O1	0.95	2.55	3.288(3)	135	1-x, -y, 1-z
C2–H2···N10	0.95	2.57	3.451(5)	155	2-x,-y,1-z
C11···H11A···N10	0.98	2.61	3.517(5)	154	-1+x, y, z
Intra C11–H11B···O1	0.98	2.39	2.989(4)	119	
C12–H12C···N7	0.98	2.52	3.429(4)	154	1-x,-y,-z
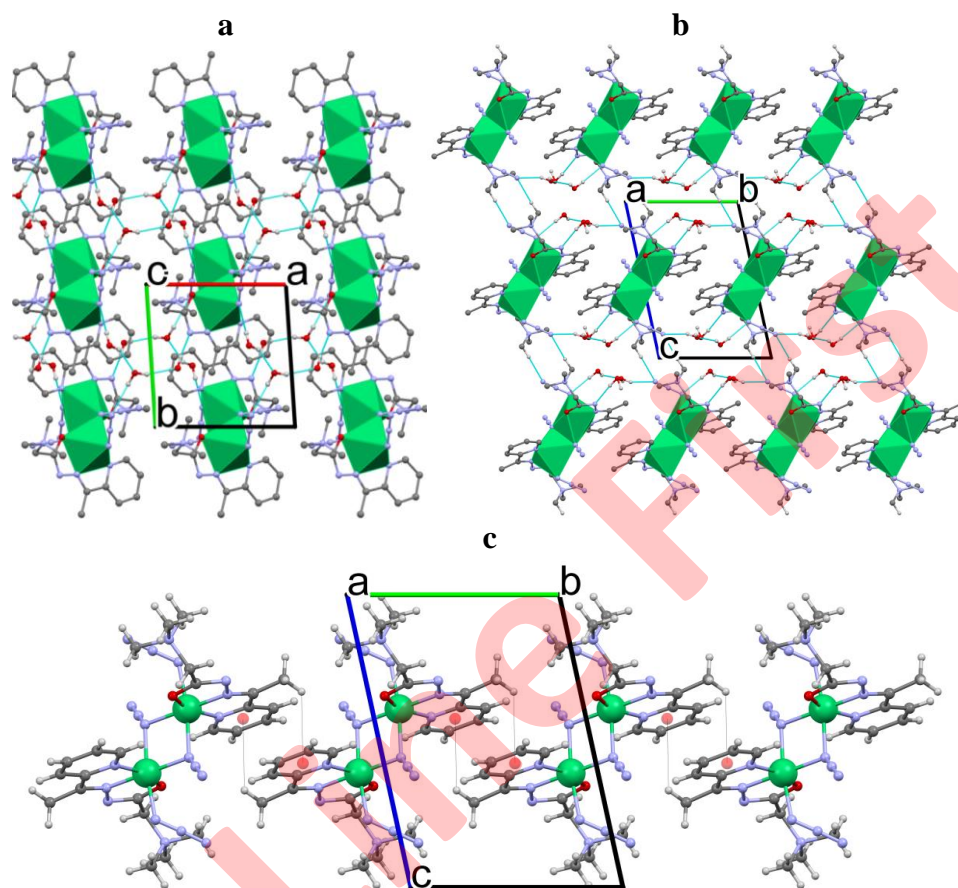
Fig S-1. Crystal packing of **1** showing a) 2D layer parallel with the (001) lattice plain generated by intermolecular hydrogen bonding. b) Side view of the layers parallel with the (001) lattice plane showing channels propagating parallel with *a* axis filled with solvent water molecules. Hydrogen atoms have been omitted for the sake of clarity, except those involved in hydrogen bonding. c) C7–H7B···π(py) intermolecular contact connecting dimers of **1** along [010] direction.